Supplementary Information

Photocatalytic Hedgehog Particles for High Ionic Strength Environments

Douglas Montjoy[1], Harrison Hou[1], Joong Hwan Bahng[2], Aydin Eskafi[1], Ruiyu Jiang[3],

Nicholas A. Kotov[1-4]

[1]Department of Chemical Engineering, [4]Department of Biomedical Engineering, [5]Department of Materials Science, and [6]Biointerfaces Institute, University of Michigan, Ann Arbor, Michigan 48109, United States;

[2] Department of Electrical Engineering, California Institute of Technology, Pasadena, California 91125, USA;

[3] Jiangsu Collaborative Innovation Center for Ecological Building Material and Environmental Protection Equipment, Yancheng Institute of Technology, Yancheng 224051, China;

*E-mail: kotov@umich.edu

Calculation of Electric Field Strength

The spherical Poisson-Boltzmann equation for the electric potential around a spherical particle in in a electrolyte solution[1,2] was computed to estimate the electric field. A particle with a constant surface charge density, σ, independent of the electrolyte concentration was assumed.[2] The equation for a 1:1 electrolyte is displayed below.[2]

$$\sigma = \frac{2\pi\varepsilon_0\varepsilon_r k_b \kappa T}{ze}\sinh\left(\frac{ze\zeta_{ZnO}}{2k_bT}\right)\sqrt{1+\frac{1}{\kappa a}\frac{2}{cosh^2\left(\frac{ze\zeta_{ZnO}}{4k_bT}+1\right)}^2+\frac{1}{\kappa a^2}\tanh\frac{8\ln\left[\cosh\left(\frac{ze\zeta_{ZnO}}{4k_bT}\right)\right]}{\sinh^2\left(\frac{ze\zeta_{ZnO}}{2k_bT}\right)}}$$

Where ε_0 is the permittivity of vacuum, ε_r is the dielectric constant of the media, *e* is electric charge in Coulombs, *a* is the particle radius, and ζ_{ZnO} is the zeta potential in water (experimentally measured ζ_{ZnO} =13.0 mV). Solutions were also computed as a function of zeta potential. κ represents the reciprocal double layer thickness and is given by:

$$\kappa = \sqrt{\frac{1000N_A e^2}{\varepsilon_0\varepsilon_r k_b T}\Sigma_i M_i x Z_i^2}$$

where N_A is Avogadro's number, k_b – Boltzman constant, M_i and Z_i are the molar concentration and valency of ions, respectively. For computation of the Debye length of the water/acetonitrile (ACN) mixture, the concentration of ions was assumed to be extremely dilute (10^{-7} M) with an estimate of the adjusted dielectric constant (ε = 64.7) based on the 2:1 mixture, which is very close to literature value. An extremely dilute concentration of ions (10^{-7} M) was also assumed for calculation of Debye length of pure ACN. For the dielectric constant of 1 M NaCl/ACN and 1M $MgCl_2$/ACN solutions, literature values were used for the dielectric constant of the salt solutions,[3,4] and then adjusted and estimated for the 2:1 mixture with acetonitrile. HPs were analyzed as spheres with diameters equivalent to the total core + shell diameter. In this case, shifting the size of the HP has little effect on the overall electric field.

For 1 M $MgCl_2$, the electric potential around a spherical particle was estimated using an analytical expression derived by Oshima et al. for 2:1 electrolytes.[1]

$$p = 1 - exp\left(-\frac{e\zeta_{ZnO}}{k_bT}\right)$$

$$q = \left(\frac{2}{3}exp\left(\frac{e\zeta_{ZnO}}{k_bT}\right)+\frac{1}{3}\right)^{1/2}$$

$$\sigma = \frac{\varepsilon_r\varepsilon_0 k_b \kappa T}{e}\left(pq+\frac{2[(3-p)q-3]}{\kappa apq}\right)$$

.

Where ε_0 is the permittivity of vacuum, ε_r is the dielectric constant of the media, *e* is electric charge in Coulombs, and ζ_{ZnO} is the zeta potential of ZnO nanorods (NRs) in water (experimentally measured as ζ_{ZnO} = 13.0 mV. The surface charge densities were converted to electric fields outside the particle by the equation below where ε_r refers to the solvent environment (r > R; in **Figure 4C** r = R+Å)

An exponential dampening term was added to account for screening due to the high ionic strength.

$$E = \frac{\sigma}{\varepsilon_0 \varepsilon_r} * \frac{R}{r} * e^{-\kappa r}$$

NRs were compared to HPs, by characterizing the size of the NRs in terms of a sphere with an effective radius (94.2 nm) given by:

$$r_{eff} = (3V/4\pi)^{1/3}$$

A similar electric field is observed for the NRs (**Figure S8**). Electric field was also calculated as a function of distance from the surface with the measured zeta potential. For high ionic strength, the field decreases exponentially, reflecting the localized electric field with little difference between HPs and NRs. At low ionic strength, a larger difference is observed and because of minimal screening, there is a smaller decrease (**Figure S9**). Surface charge densities largely reflect the electric fields observed, with some difference in acetonitrile compared to water. A higher surface charge density is observed in the latter but greater field strength with the former due to the decrease in electric field strength from the higher relative permittivity of the solvent (**Figure S8**).

Supplementary Figures

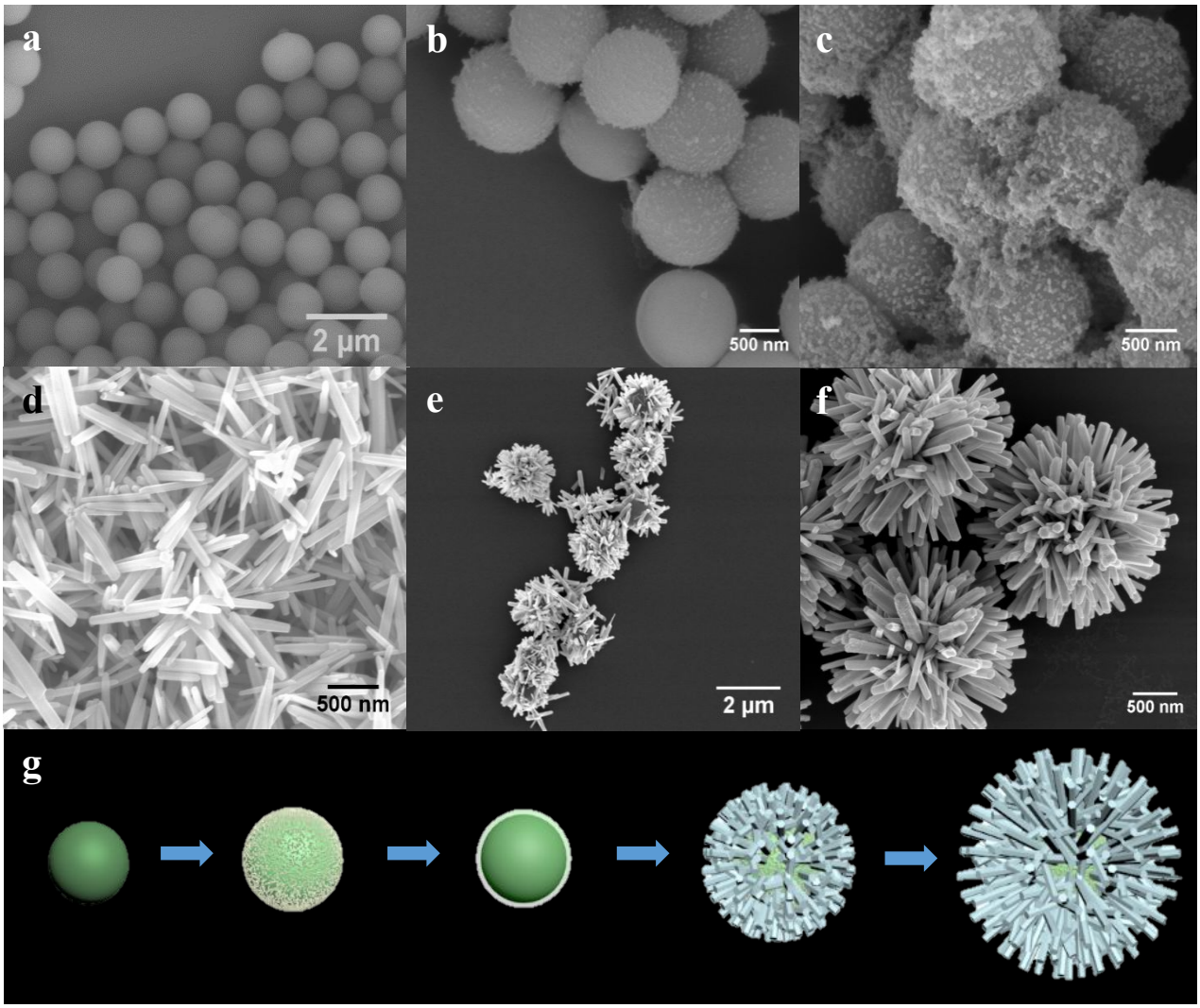

Figure S1: (**a)** SEM image of SiO_2 particles serving as the core particles for HPs synthesized using the Stöber process. Stöber SiO_2 microparticles without PAA/PAH LBL coating (**b**) and with PAA/PAH LBL (**c**) coatings after incubation with ZnO NPs for 1 hour. (**d**) ZnO NRs collected from synthesis of HPs for benchmark comparison tests. HPs made using carboxylated SiO_2 core microparticles without LBL films (**e**) and with LBL films (**f**). (**g**) Schematic showing coating of SiO_2 microparticle with LBL coating and then deposition of ZnO NPs, which are hydrothermally grown under sonication into spikes to form HPs.

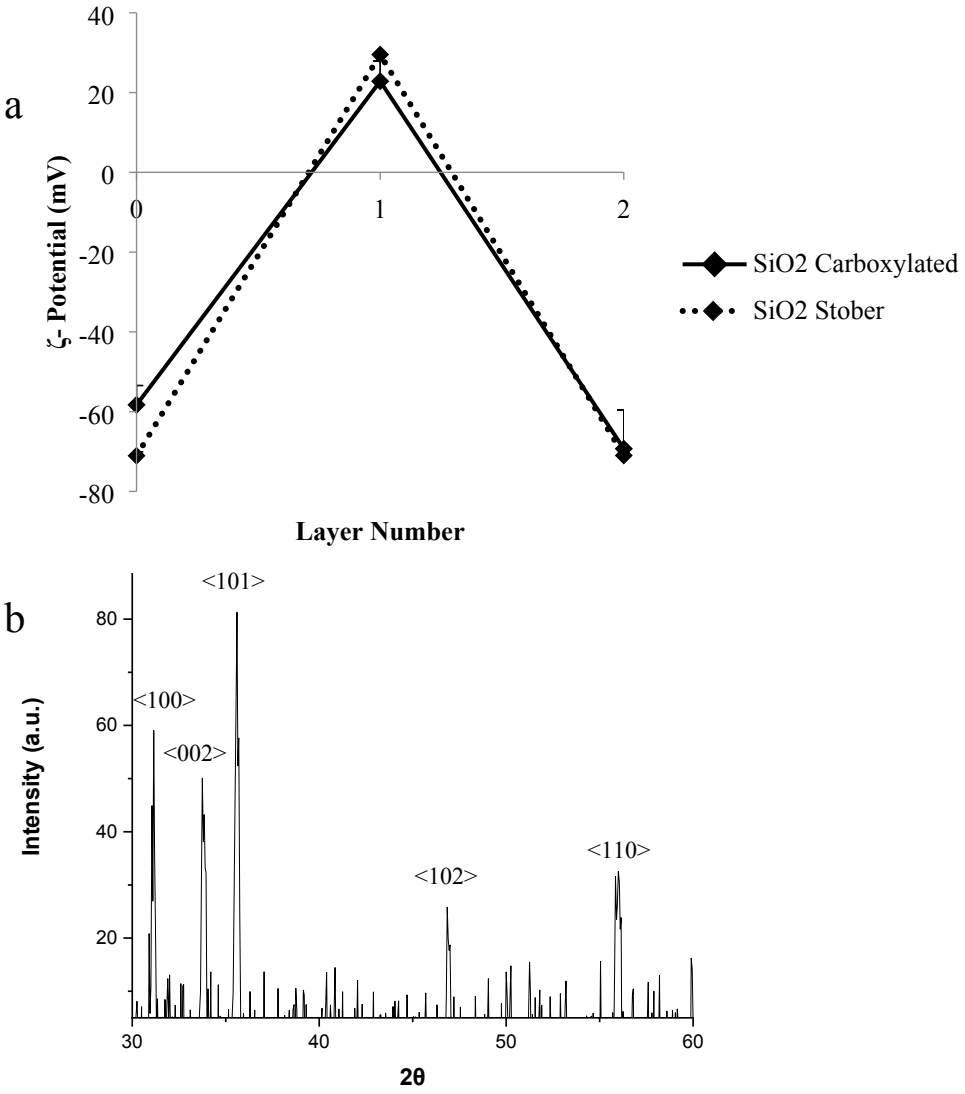

Figure S2: **(a)** Zeta potential of commercial carboxylated SiO_2 and Stöber SiO_2 microparticles as a function of polyelectrolyte layer number deposited in LBL process. (**b**) Indexed X-ray diffraction pattern of HP_{S2}.

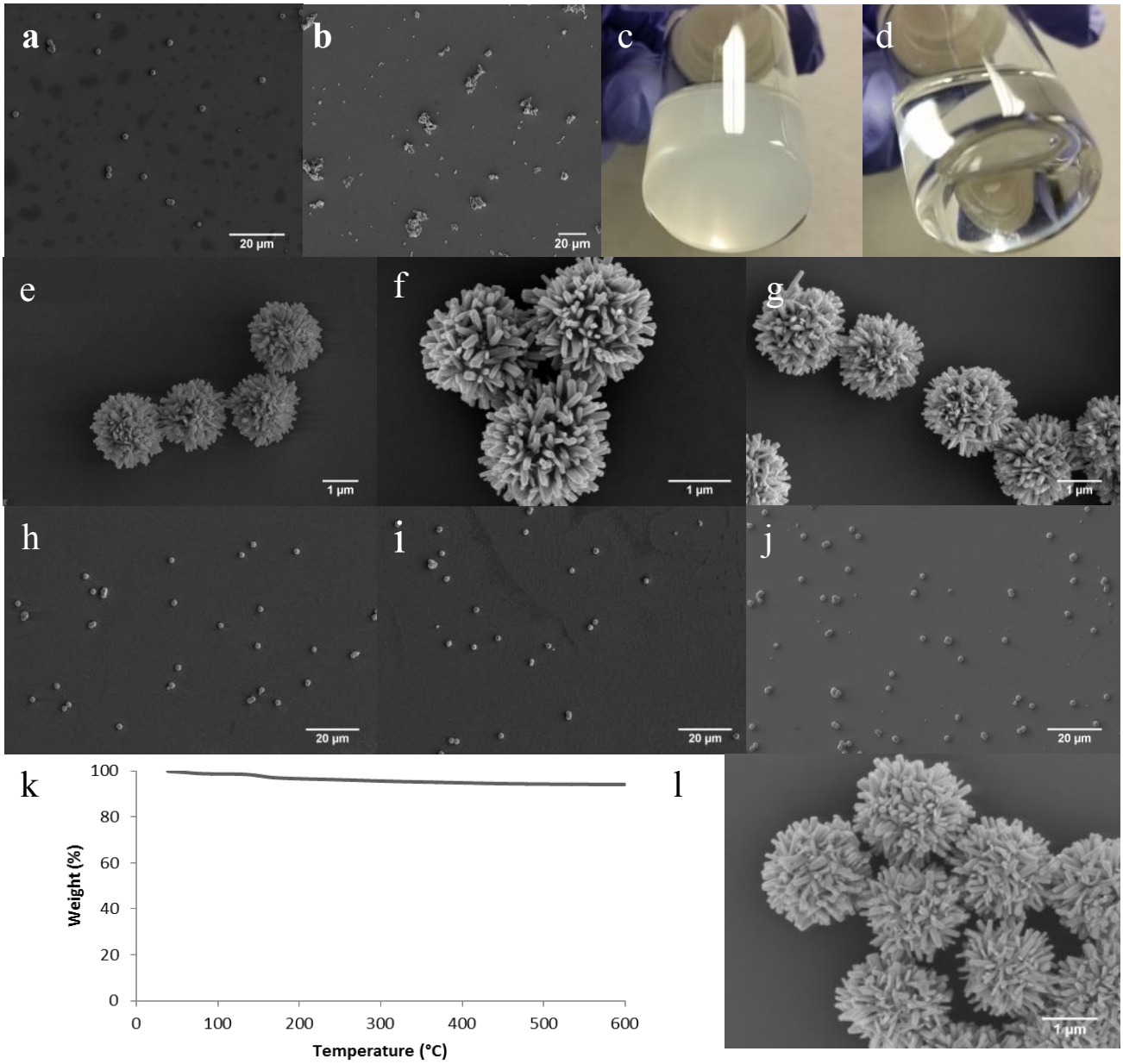

Figure S3: SEM images of SiO_2 HPs (**a**) and SiO_2 cores (**b**) dispersed in heptane (0.1 mg/mL). Photograph of sediments (0.5 mg/mL) of SiO_2 HPs (**c**) and SiO_2 cores in heptane (**d**) after 1 minute. SEM images of HPs with SiO_2 cores in chloroform (**e,h**), tetrahydrofuran (**f,i**) and toluene (**g,j**) after 1 week (0.1 mg/mL). (**k**) Thermogravimetric analysis of SiO_2 HPs (**l**) SEM image of SiO_2 HPs after treatment at 500 ºC for 24 hours.

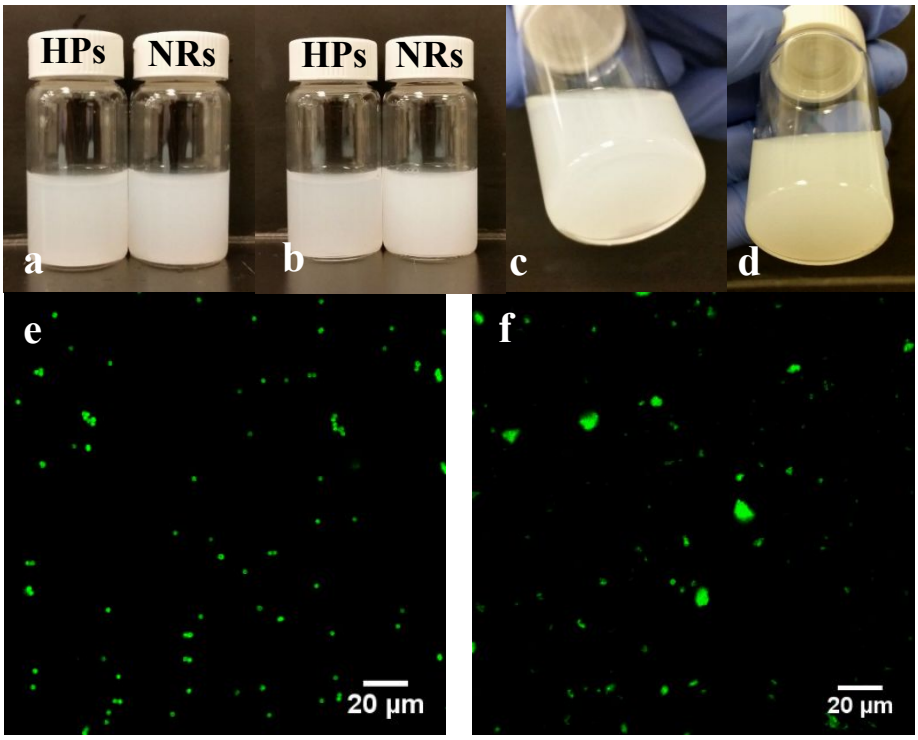

Figure S4: Photographs of dispersions of (**a**) SiO_2 HPs and ZnO nanorods (NRs) identical to nanospikes forming the spiky 'halo' of HPs in 1M NaCl (**a**) and 2M NaCl (**b**) (0.5 mg/mL). (**b**) SiO_2 HP and ZnO NR dispersions in 2M NaCl (0.5 mg/mL). Photographs of sediment of SiO_2 HPs (**c**) and NRs (**d**) in 1M NaCl (0.5 mg/mL) after 1 minute. Confocal microscopy images of SiO_2 HPs (**e**) and ZnO NRs (**f**) dispersed in 1M NaCl (0.1 mg/mL).

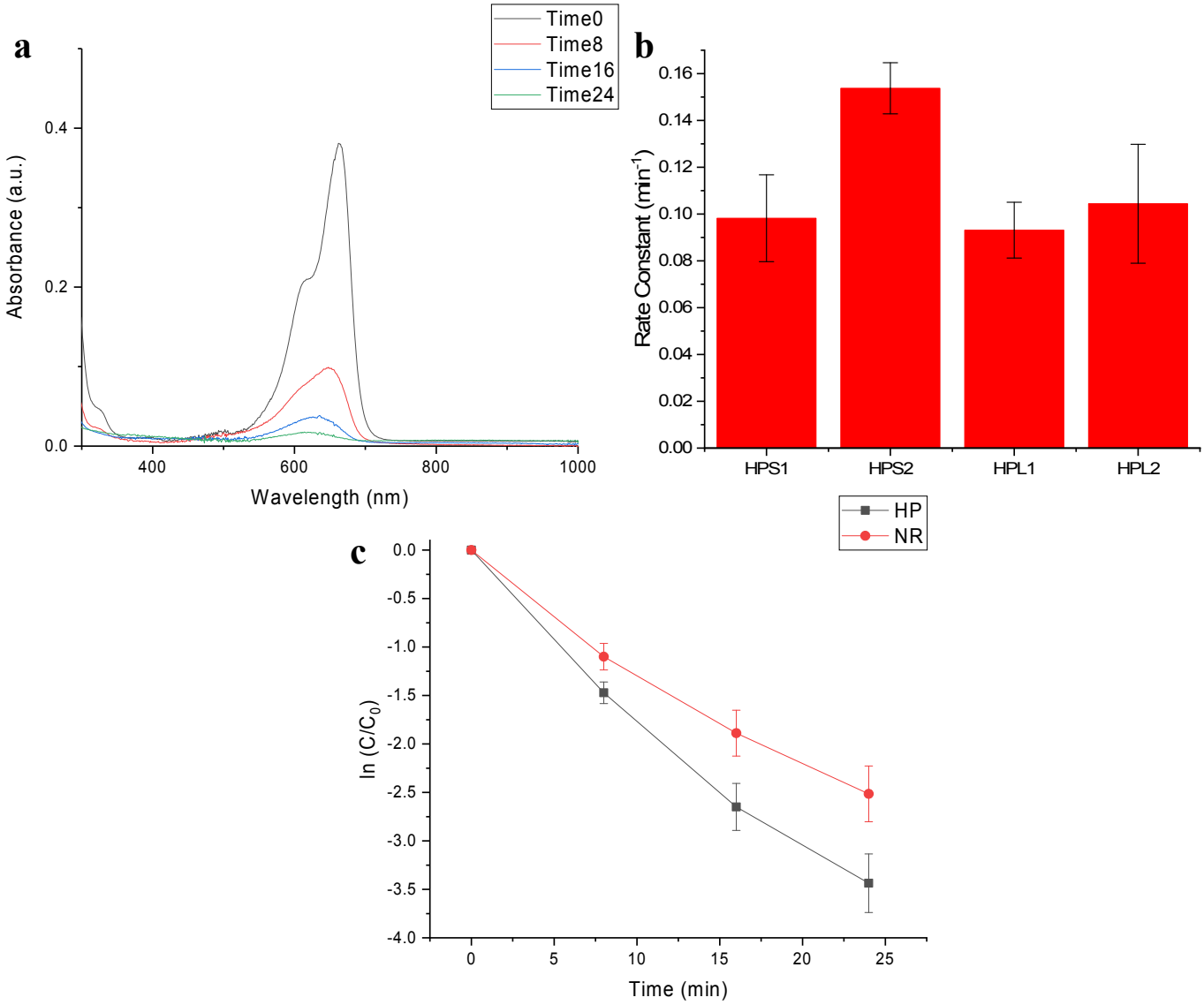

Figure S5: (**a**) Spectral changes of MB solution (5 x 10^{-5} M) upon photo-degradation catalyzed by HP_{S2}. (**b**) Rate constants in MB photooxidation for different HPs with different spike lengths and widths; geometrical parameters are given in **Table S1**. (**c**) Photodegradation Kinetics of MB (5 x 10^{-5} M) in water by ZnO NRs and HP_{S2}. The catalyst concentration was 2 mg/mL and a 302 nm UV source was used for all the experimental sets.

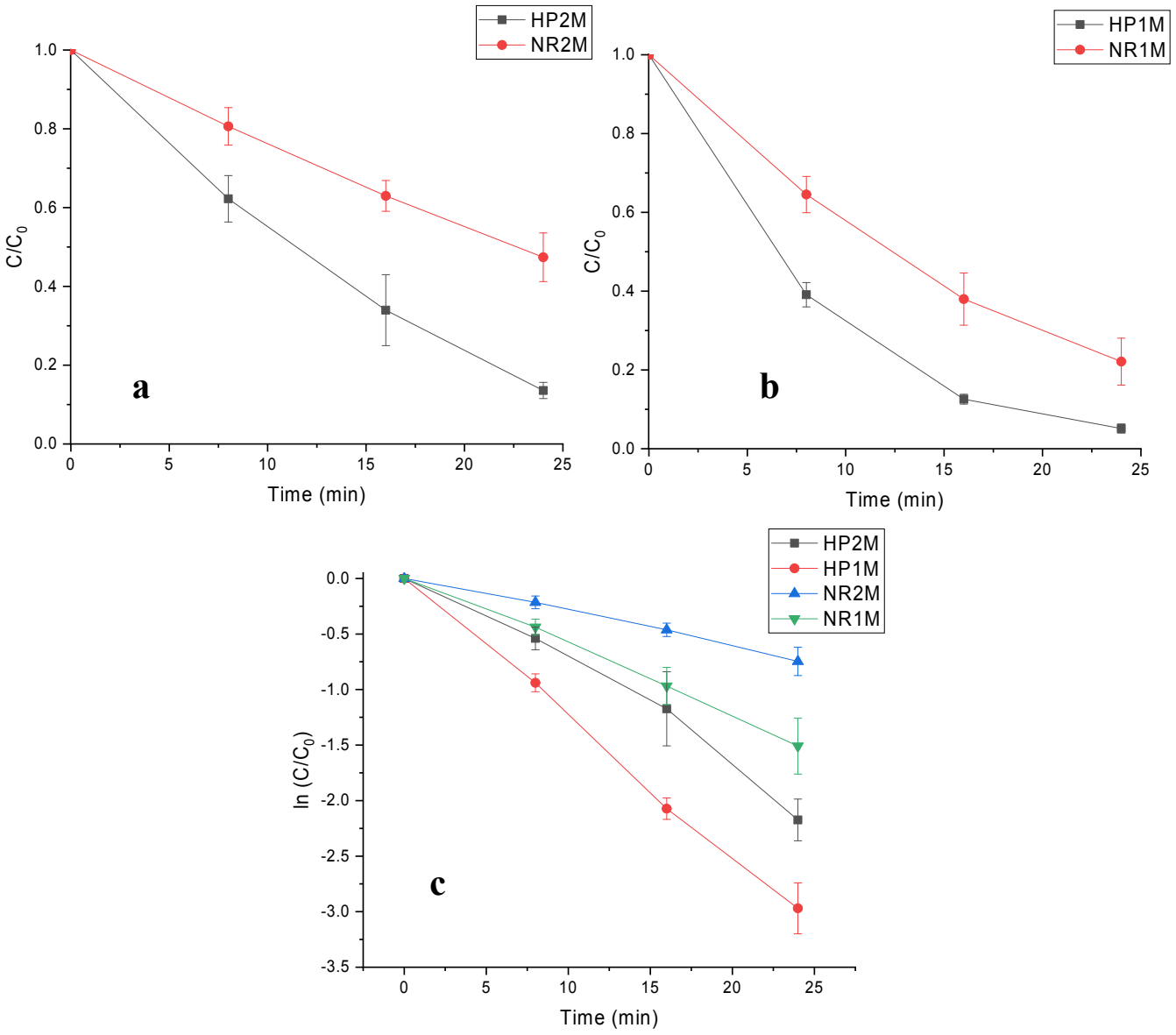

Figure S6: Degradation of MB (5 x 10^{-5} M) in 1M NaCl (**a**) and 2M NaCl (**b**) by ZnO NRs and HP_{S2}. Photodegradation kinetics of MB for different NaCl concentrations with HP_{S2} and ZnO NR catalysts (**c**). The concentration of all catalysts was 2 mg/mL a 302 nm light source was used.

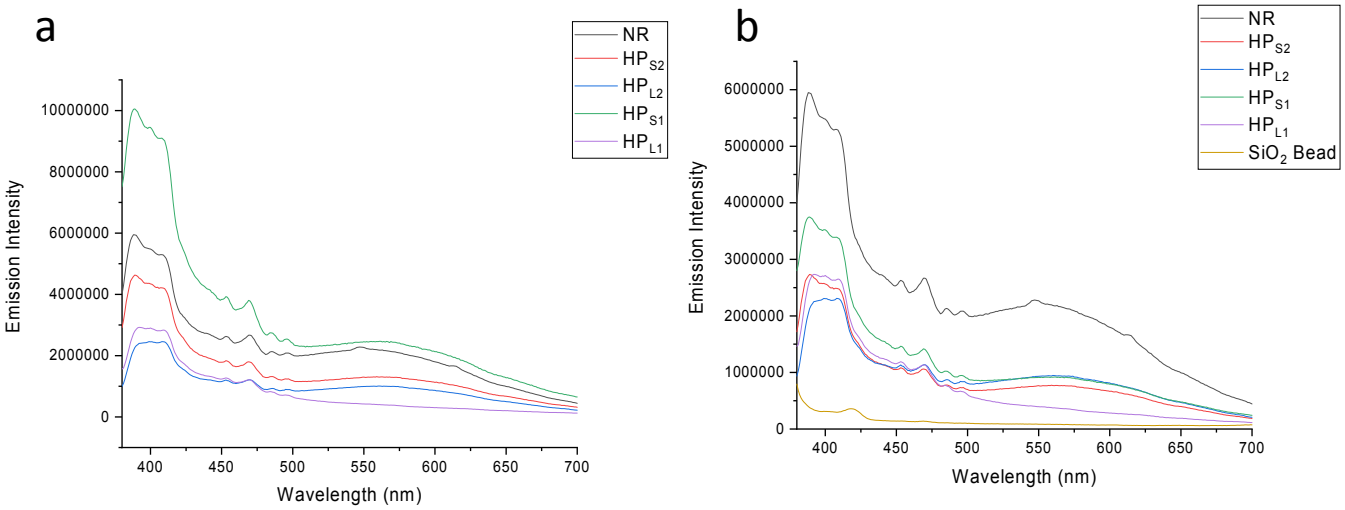

Figure S7: Photoluminescence spectra with excitation of 360 nm of HP samples and ZnO nanorods normalized by estimated ZnO content (**a**) and without normalization (**b**). Measured spike length and width in **Table S1** were used with a total of 200 spikes per HP to estimate the content.

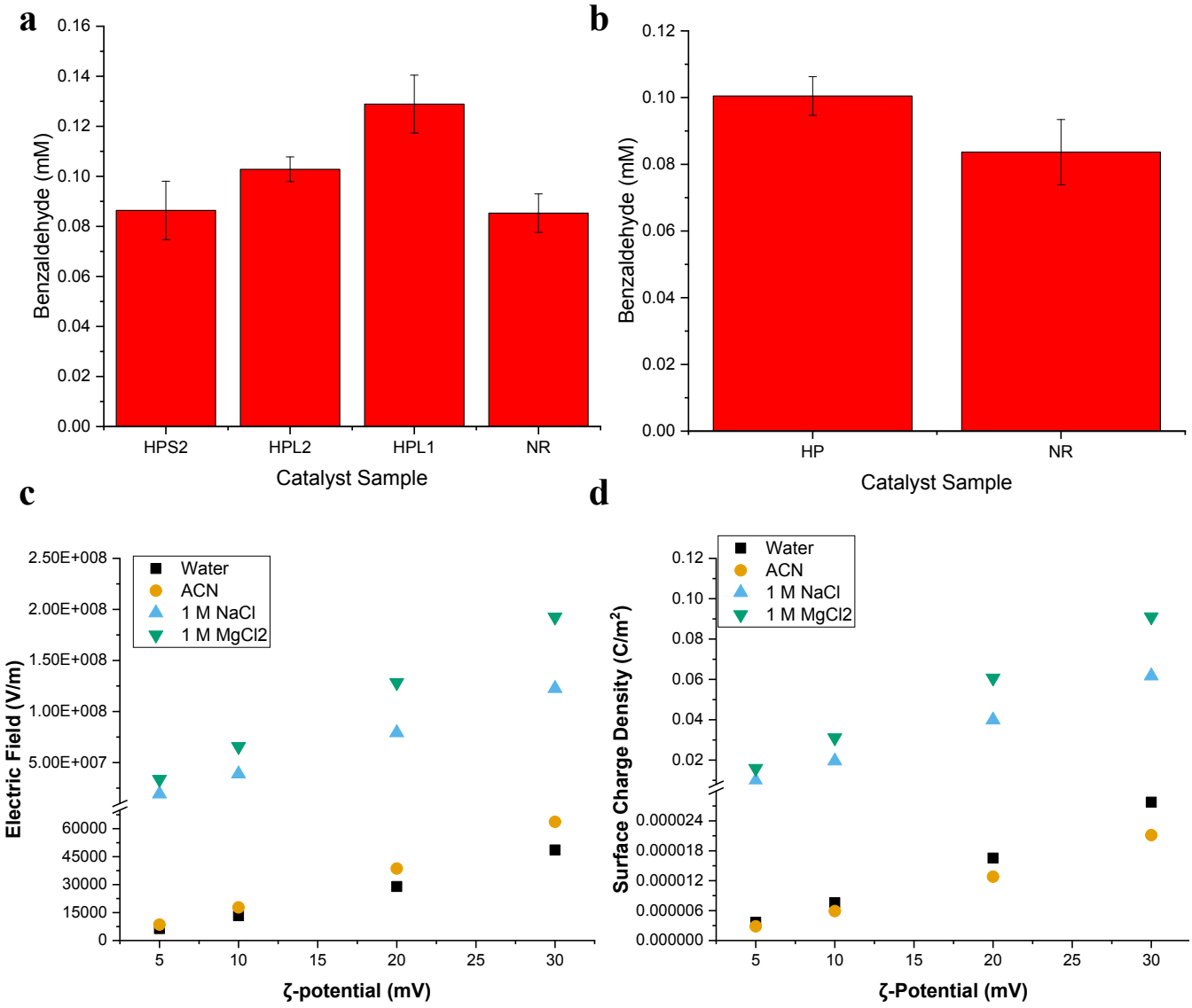

Figure S8: **(a)** Production of benzaldehyde from photooxidation of 2-phenoxy-1-phenylethanol (PP-ol) for 2 hours with a 302 nm light source with different heterogeneous catalysts added in the amount of 3 mg/mL in 1M $MgCl_2$/ACN (2:1 ratio). (**b**) Production of benzaldehyde from photooxidation of PP-ol for 2 hours with HP_{L1} and NRs added in the amount of 3 mg/mL in 1M $CaCl_2$/ACN (2:1 ratio). A 302 nm light source (8 W) was used. (**c**) Electric field strength for ZnO nanorods treated as spheres with effective radius (94.2 nm) and (**d**) surface charge density for ZnO HPs calculated utilizing DLVO theory and the Poisson-Boltzmann equation for a spherical particle in aqueous and salt mixtures with ACN (2:1) and pure ACN as a function of ζ

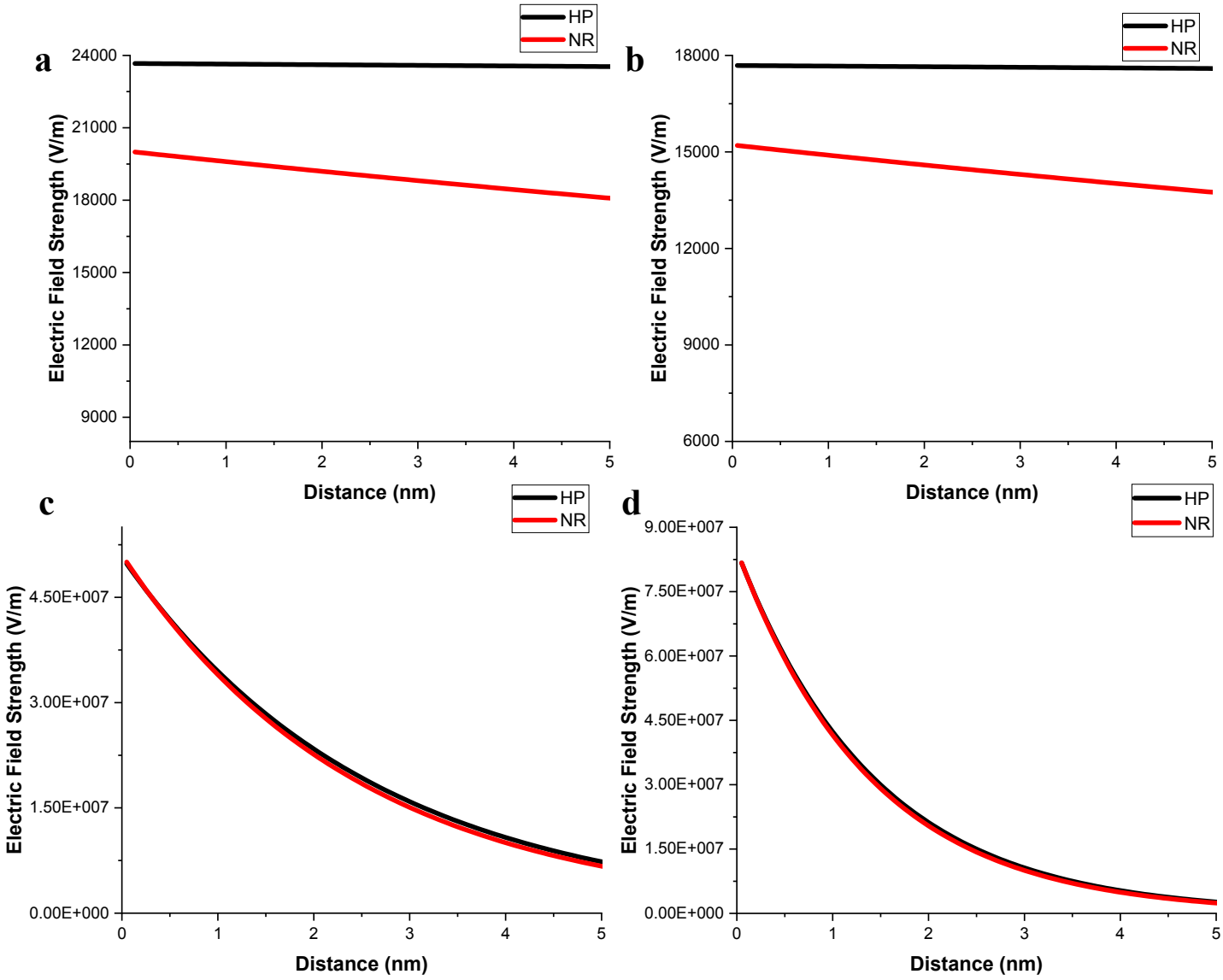

Figure S9: Electric field strength for HPs and ZnO nanorods (treated as spheres with effective radius (94.2 nm)) calculated utilizing DLVO theory and the Poisson-Boltzmann equation for a spherical particle. In water/ACN (**a**), Pure ACN (**b**), 1 M NaCl/ACN (**c**), and 1 M $MgCL_2$/ACN (**d**) as a function of radius with measured ζ-potential=13.0 mV (see DLVO Calculation of Electric Field).

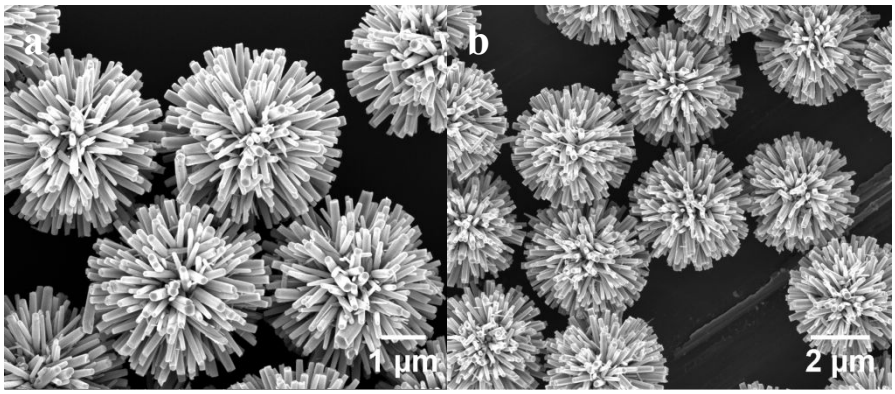

Figure S10: SEM images of HP_{L1} catalyst after photoreaction in 1 M $MgCl_2$ in H_2O/ACN (**a**) and in 1 M $TBAPF_6$ (**b**) in ACN.

Table S1: Spike width, length, and total diameter of HPs synthesized using different precursor concentrations and number of spike growth stages (that can also be referred to as number of sonication times).

HP	Spike Width (nm)	Spike Length (nm)	Total Diameter (nm)	Precursor Concentration (mM)	Number Of Spike Growth Stages
HP_{S1}	58 ± 14	482 ± 63	2091 ± 127	25	1
HP_{S2}	72 ± 17	758 ± 56	2643 ± 113	37.5	1
HP_{L1}	166 ± 27	1545 ± 240	4216 ± 480	37.5	2
HP_{L2}	146 ± 25	1864 ± 122	4855 ± 244	25	2

Table S2: BET surface area measurements and zeta potential measurements of HPs and ZnO NR catalysts.

Catalysts	**Surface Area (m^2/g)**	**Zeta Potential (mV)**
ZnO NR	11.76 ± 0.007	13.0 ± 3.5
HP_{S1}	6.14 ± 0.098	-19.9 ± 0.71
HP_{S2}	8.65 ± 0.037	-18.9 ± 1.7
HP_{L1}	5.20 ± 0.015	-15.4 ± 4.8
HP_{L2}	8.20 ± 0.017	-23.2 ± 2.1

Supplementary References

(1) Ohshima, H.; Healy, T. W.; White, L. R. Accurate Analytic Expressions for the Surface Charge Density/Surface Potential Relationship and Double-Layer Potential Distribution for a Spherical Colloidal Particle. *J. Colloid Interface Sci.* **1982**, *90* (1), 17–26. https://doi.org/10.1016/0021-9797(82)90393-9.

(2) Makino, K.; Ohshima, H. Electrophoretic Mobility of a Colloidal Particle with Constant Surface Charge Density. *Langmuir* **2010**, *26* (23), 18016–18019. https://doi.org/10.1021/la1035745.

(3) Jia, G. Z.; Liu, S.; Liu, F. H.; Liu, J. C. Ion–Water Cooperative Interactions in Aqueous Solutions of $MgCl_2$ by Dielectric Spectroscopy. *J. Dispers. Sci. Technol.* **2016**, *37* (1), 1–5. https://doi.org/10.1080/01932691.2015.1010728.

(4) Buchner, R.; Hefter, G. T.; May, P. M. Dielectric Relaxation of Aqueous NaCl Solutions. *J. Phys. Chem. A* **1999**, *103* (1), 8–9. https://doi.org/10.1021/jp982977k.

(5) Yu, B.; Cong, H.; Xue, L.; Tian, C.; Xu, X.; Peng, Q.; Yang, S. Synthesis and Modification of Monodisperse Silica Microspheres for UPLC Separation of C60 and C70. *Anal. Methods* **2016**, *8* (4), 919–924. https://doi.org/10.1039/C5AY02655E.